Control of PbSe Quantum Dot Surface Chemistry and Photophysics Using an Alkylselenide Ligand

Barbara K. Hughes,[†,‡] Daniel A. Ruddy,[‡] Jeffrey L. Blackburn,[‡] Danielle K. Smith,[‡] Matthew R. Bergren,[‡,§] Arthur J. Nozik,[†,‡] Justin C. Johnson,[‡,*] and Matthew C. Beard[‡,*]

[†]Department of Chemistry and Biochemistry, University of Colorado, Boulder, Colorado 80309, United States, [‡]Chemical and Materials Science Center, National Renewable Energy Laboratory, Golden, Colorado 80401, United States, and [§]Department of Physics, Colorado School of Mines, Golden, Colorado 80401, United States

ABSTRACT

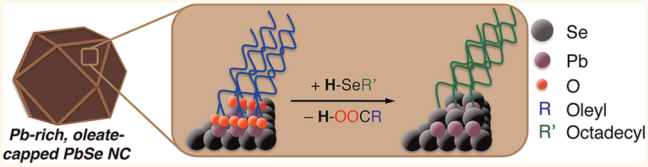

We have synthesized alkylselenide reagents to replace the native oleate ligand on PbSe quantum dots (QDs) in order to investigate the effect of surface modification on their stoichiometry, photophysics, and air stability. The alkylselenide reagent removes all of the oleate on the QD surface and results in Se addition; however, complete Se enrichment does not occur, achieving a 53% decrease in the amount of excess Pb for 2 nm diameter QDs and a 23% decrease for 10 nm QDs. Our analysis suggests that the Se ligand preferentially binds to the {111} faces, which are more prevalent in smaller QDs. We find that attachment of the alkylselenide ligand to the QD surface enhances oxidative resistance, likely resulting from a more stable bond between surface Pb atoms and the alkylselenide ligand compared to Pb-oleate. However, binding of the alkylselenide ligand produces a separate nonradiative relaxation route that partially quenches PL, suggesting the formation of a dark hole-trap.

KEYWORDS: quantum dots · photoluminescence · nuclear magnetic resonance · lead chalcogenides · nanoparticles

Precise control over quantum dot (QD) surfaces is an ongoing research challenge that, if solved, should lead to a broader impact of QDs in many technological areas. Recent studies have demonstrated that photophysical properties such as photoluminescence (PL),[1,2] carrier mobility,[3,4] and multiple-exciton generation (MEG)[5,6] can depend on the QD surface composition. A better understanding of the QD–ligand interaction and its relation to surface chemistry will enable greater control of photophysical properties. As an example, modifying QD surface chemistry by employing surface treatments to lead chalcogenide (PbX, X = S, Se) QDs has produced QD films for use in next-generation photovoltaic structures that have achieved power conversion efficiencies greater than 4%.[7] Quantum-confined semiconductors offer numerous advantages over bulk semiconductors for the design of novel optoelectronic applications such as low-cost solution processing[8] and enhanced MEG. Further advances will necessarily involve better control over the surface defect states and their passivation.[9]

Though PbSe QDs are often modeled as quasi-spheres, their surfaces are in fact multifaceted, and the relative contribution of different facets changes with particle size and synthetic conditions. The {111} and {100} faces of the PbX rock salt crystal structure are usually assumed to dominate the QD surface. Under this assumption, the faceted nature follows that of a truncated cube. The smallest QDs (~1–3 nm) exhibit the most spherical nature and are likely truncated octahedra dominated by 8-{111} faces. As the QDs continue to grow into a size regime between ~3 and 8 nm, the interplay between growth along the ⟨111⟩ and ⟨100⟩ directions favors the lower surface energy {100} faces over the higher energy {111} faces and a cuboctahedron results in crystal termination with roughly equal contributions from the {100} and {111} faces. Other faces such as the {110} may also be present and recently were postulated to be responsible for oriented growth of Pb-chalcogenide quantum sheets.[10] In the QD core, (111) planes alternate between all Pb and all Se atoms, while the (100) and (110) planes are stoichiometric. The actual structure of the QDs likely deviates from this simple picture, especially for smaller QDs with a larger number of exposed facets, leading to reconstructed lattice planes, as recently observed in CdSe QDs[11] and calculated for PbSe QDs.[12,13] Atomistic calculations show that the surface

* Address correspondence to Matt.Beard@nrel.gov Justin.Johnson@nrel.gov.

Received for review March 30, 2012 and accepted May 9, 2012.

Published online May 09, 2012
10.1021/nn301405j

energies of the various facets can vary depending on Pb *vs* Se termination, how the atoms are arranged on the surface (*i.e.*, atomically flat *vs* nanofaceted regions on the larger faces), and the ligand that terminates the QD.[14] Assuming that surface atoms are mobile at room temperature, the particle faces will rearrange to achieve the lowest possible surface free energy, with the stoichiometric {100} face having the lowest surface energy. At the largest sizes, PbSe QDs are known to undergo a sphere-to-cube transition in which all faces are terminated by {100} surfaces.[12,13,15−17] The quasi-sphere-to-cube transition depends upon the growth conditions along the ⟨100⟩ and ⟨111⟩ directions and should reflect the relative reactivity of the anion precursor. While the precise contribution of different facets is difficult to determine, interesting studies have shown that the interplay between ligand−ligand and ligand−solvent interactions along with the underlying QD morphology can be employed to tune different QD superlattice configurations.[18]

Several research groups have found that as-made PbSe QDs are significantly cation-rich.[15,19,20] Moreels *et al*. introduced a model of a typical PbSe QD where the core is stoichiometric while all surface Se atoms are terminated by Pb, resulting in a Pb-rich QD where the calculated Pb:Se ratios match the values measured using analytical techniques.[19] Moreels *et al*. further measured a Pb_{excess}:oleate ratio of ∼1, and when accounting for all surface Pb, this results in two surface Pb atoms per one oleate ligand.[21] Therefore, excess Pb surface atoms are not compensated by the −1 charge assigned to the oleate ligand assuming each Pb has a +2 charge and each Se a −2 charge. Recent DFT calculations support this 2:1 $Pb_{surface}$:acid anion ratio for both the {100} and {111} faces as the most stable Pb-carboxylic acid bonding configuration.[16−18,22]

Altering the anion/cation ratio at the QD surface has been shown to affect both photophysical and electrical properties and may influence QD film performance. For instance, PbSe QD films treated with 1, 2-ethanedithiol (EDT) exhibit p-type transport behavior, while hydrazine-treated films exhibit n-type behavior.[23] EDT treatment of films produces an anion-rich environment, while hy-treated films retain the cation-rich nature of the as-prepared QDs (see Figure 2 for details). This is consistent with the behavior of bulk PbSe, where Pb vacancies lead to p-type behavior, while Se vacancies exhibit n-type behavior.[24] Midgap surface states that could serve as carrier trap sites are also highly dependent on the QD−ligand structure. Stoichiometric, ligand-free QDs do not have midgap states.[12,17,25] However, nonstoichiometric QDs and those with ligands could have midgap surface states that serve as carrier trap sites, which would be highly dependent on the QD−ligand structure.[12,17] A better understanding of QD−ligand interactions and control over QD surfaces will enable a greater ability to tailor electrical properties of these functional QD solids.

Here we report the successful addition of Se atoms to the surface of PbSe QDs and the resulting changes to the photophysical properties that arise from shifting away from Pb-oleate termination. Se atoms are attached to the QD surface with sufficient passivation in the form of an alkylselenide ligand. The alkylselenide reagents can be used directly in the preparation of PbSe QDs or as a postsynthetic treatment to exchange surface oleate ligands. Low-temperature PL spectroscopy reveals that addition of the alkylselenide ligand significantly reduces nonradiative surface trap sites associated with oxidation, presumably through a strong, relatively stable $Pb_{surf}-SeC_{18}H_{37}$ interaction. We demonstrate that the oxidation rate of PbSe films is reduced by the addition of the alkylselenide ligand. In addition, a new Se-related trap state arises following treatment, as evidenced by a decrease in photoluminescence quantum yields (PLQYs).

RESULTS AND DISCUSSION

Aklyselenide Synthesis and QD Addition. Similarly to work by Jasieniak *et al*.[26] on Se-treated CdSe, we successfully prepared anion-rich PbSe QDs with an overall Pb/Se ratio of 0.96 through the addition of trioctylphosphine selenide (TOP-Se) to oleate-capped QDs. The resulting QDs were stable in excess TOP-Se, and a layer of Pb could be added to the QD surface by introduction of $Pb(oleate)_2$. However, in this case the PL properties continually degraded upon successive addition of Pb and Se. In contrast to CdSe QDs, excess TOP leads to vibrational signatures that mask the optical excitonic signatures of the PbSe QDs, and therefore removing excess TOP is important. However, after several washes to remove excess TOP-Se, the resulting QDs precipitated presumably due to nonligated surface Se atoms. In order to increase the anion/cation ratio of PbSe and retain colloidal stability, we found it necessary to develop a methodology that incorporates a solubilizing group with the large Se anion at the particle surface, which, unlike TOP, will not leave as a neutral molecule upon washing.

Two alkylselenide reagents were prepared from adapted literature procedures, dioctadecyl diselenide, $[CH_3(CH_2)_{17}Se]_2$ (**1**), and octadecylselenol, $CH_3(CH_2)_{17}SeH$ (**2**).[27] The selenol **2** was determined to be the active species for Pb_{surf}−oleate exchange *via* proton transfer from **2** to form free oleic acid and a $Pb_{surf}-SeC_{18}H_{37}$ group (Figure 1). The diselenide **1** is easily transformed *in situ* to **2** through the use of 1 equivalent of diphenylphosphine (DPP) as a reductant, analogous to the well-known reaction of secondary phosphines with disulfides.[28] Although **2** exhibited fast ligand exchange reactivity (1−2 min), due to its potential instability toward air and moisture, the air-stable diselenide **1** was used for the bulk of the surface chemistry reported here and is convenient in the

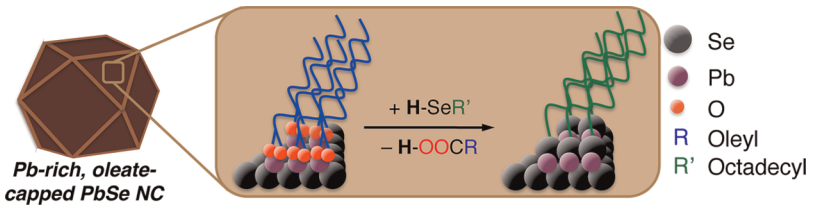

Figure 1. Surface exchange of Pb-oleate-capped QDs for a Se-terminated surface *via* proton transfer from selenol to produce free oleic acid.

procedures developed here due to the presence of DPP (or other secondary phosphines) in PbSe QD preparations.

Alkylselenide-terminated QDs are produced using two methods. The first method utilizes an *in situ* selenide termination *via* a two-injection synthesis procedure beginning with a solution of $Pb(oleate)_2$ (from lead oxide and oleic acid). The first injection solution is the commonly employed trioctylphosphine selenide with 0.08 equivalent of DPP *vs* Se to nucleate and grow oleate-capped PbSe QDs at 160 °C. After the desired growth time is reached, a second injection of **1** in chloroform is added. After 20 s the solution is rapidly cooled, and the alkylselenide-capped PbSe QDs are isolated *via* repeated precipitations from hexane with ethanol. Alternatively, traditionally prepared and isolated oleate-capped PbSe QDs can be treated with **1** (plus 1 equivalent of DPP) or **2** in hexane at room temperature. Treatment with **1**/DPP takes 1−2 days to reach completion, at which point the alkylselenide-capped QDs precipitate. The product is isolated *via* centrifugation, redispersed in chloroform, and stored in a glovebox.

Treatment with **2** in hexane occurs rapidly, and the QDs precipitate from solution in less than 5 min. Excess **1** and **2** are both highly soluble in hexane and remain in the supernatant following isolation of the solid product (confirmed by ^{1}H NMR spectroscopy). The ratio of Pb:Se was determined by ICP methods in order to quantify the extent to which alkylselenide was added to the QD surface. Compositional analysis for as-prepared and alkylselenide-treated QDs is shown in Figure 2.

QD−Ligand Structure. The Pb:Se ratios were measured *via* ICP-AES (Figure 2) for the as-prepared (red circles) and alkylselenide-treated (black circles) QDs. The as-prepared QDs exhibit Pb:Se ratios ranging from 2.9 for the 2 nm QDs to 1.1 for the 10 nm diameter QDs. We compare our Pb:Se ratio of as-prepared QDs to those reported by Moreels *et al.*,[19] Smith *et al.*,[20] and Dai *et al.*[15] (see Supporting Information Figure S1) and find reasonable agreement despite dissimilar reaction conditions. After the ligand exchange the Pb:Se ratio decreases from 2.9 to 1.6 for the 2 nm QDs, resulting in a 53% decrease in the excess Pb, while for the 10 nm diameter QDs we observed a 23% decrease in the excess Pb. Figure 2b displays the percent decrease in the excess Pb as a function of QD size. As a comparison with the treated PbSe QD films studied for

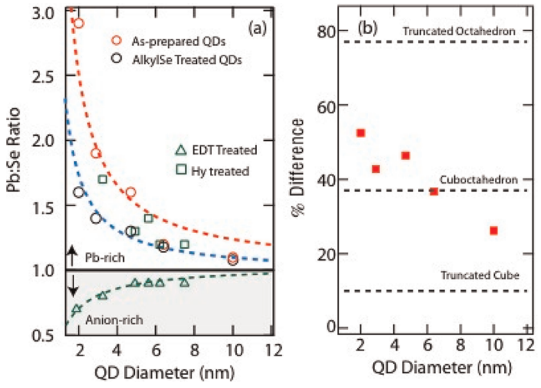

Figure 2. (a) Pb:Se ratios from elemental analysis for as-prepared (red circles) and corresponding alkylselenide-treated QDs (black circles) as a function of QD size. The red dashed line is a model assuming only Pb-terminated surfaces. The dashed blue line is a model with ~40% Se addition. We also show Pb:X ratios for conductive PbSe films prepared by EDT treatment (green triangles) or hydrazine treatment (green squares). (b) Percent decrease in the excess Pb after alkylselenide treatment; dashed lines are for truncated octahedron, cuboctahedron, and truncated cube models.

optoelectronic applications such as absorber layers in QD-based solar cells, we plot the Pb:Se ratios for hydrazine- (green squares) and EDT-treated (green triangles) PbSe QD films. We find that the Pb:Se ratio for the hydrazine-treated films is about the same as for untreated QDs, but upon treatment with EDT, the Pb:X (X = Se + S) ratio for the resulting film becomes anion-rich.

For a given morphology the Pb:Se ratio can be estimated by determining the number of excess Pb atoms (N^{Pb}_{excess}) and comparing that to the total number of atoms within the stoichiometric core (N_{core}) by the following: $Pb:Se = 1 + (2N^{Pb}_{excess}/N_{core})$. N^{Pb}_{excess} is found by calculating the number of Pb atoms in one monolayer and dividing by 2 to account for the 1/2 Pb surface coverage of a stoichiometric QD. This expression can be reduced to the following for any of the proposed morphologies: $Pb:Se = (d + a)^3/d^3$ (see Supporting Information and the red-dotted line in Figure 2a), where d is the quantum dot diameter and a is the PbSe lattice constant (0.61 nm), which corresponds to twice the average outer layer thickness of 0.3 nm. We can account for addition of Se by introducing the parameter f, which represents the degree of Pb- or Se-termination ($f = 1$ is complete Pb-termination and $f = 0$ is complete Se-termination) by the following: $Pb:Se = (1 - f) + f(d + a)^3/d^3$. The value of f can be

estimated by considering the faceted nature of the QDs and how the Pb:Se ratio would change for the following shapes: octahedron, truncated octahedron, cuboctahedron, and truncated cube. All morphologies predict the same Pb:Se ratio of the untreated or completely Pb-enriched surfaces, as noted above. However, the Se-enriched QDs will show differences if we assume that the alkylselenide ligand preferentially binds to one face because the ratio of the {111} and {100} faces depends on the morphology. We tentatively conclude that the alkylselenide ligand binds preferentially to the {111} faces by the following observation: When the alkylselenide ligand is used as the sole Se source during PbSe QD synthesis, large hexapods result (see Figure S2). Hexapods result from continued growth along the 6-{100} faces and hindered growth along the 8-{111} faces. We propose that this hindered growth is due to preferential alkylselenide ligand binding on the {111} faces. The resulting hexapod morphology is in contrast to the growth dynamics observed under normal synthesis conditions (using TOP-Se) for Pb-oleate-terminated QDs, where TEM analysis consistently finds that smaller QDs are quasi-spherical, while larger QDs are cubic. Cubes result because the {111} faces are favored during growth over the {100} faces. We, therefore, assume in the following that alkylselenide addition to oleate-terminated QDs adds Se primarily to the {111} faces. Since complete alkylselenide surface coverage does not occur, the Pb-enriched {100} faces must dominate the underlying QD morphology, and this is consistent with the cuboctahedron and truncated cube shapes. For example, a QD morphology resembling a truncated octahedron would result in a Se-rich QD after ligand exchange along the {111} face, which is not observed. These tentative conclusions are consistent with the findings of Bian *et al.*, who explain that there is a natural tendency of intermediate-sized QDs prepared by conventional synthesis conditions toward an underlying bcc superlattice structure due to the characteristic structural properties of cuboctahedron QDs.[29] An exact calculation of f can be done but involves a laborious geometry exercise and is not necessary for our conclusions. Instead we estimate f by calculating the percent surface area for the {100} surface for the different morphologies, $f = S_{100}/(S_{100} + S_{111})$, and find $f = 0.90$ for the truncated cube, $f = 0.63$ for the cuboctahedron, and $f = 0.23$ for a truncated octahedron. When $f = 0.6$ (dashed blue line), the model reproduces our data, suggesting that following treatment, ~40% of the QD surface becomes alkylselenide terminated by primarily adding Se to the {111} face. The percent change in Pb enrichment can be estimated as $(1 - f)$ and is plotted as dashed lines in Figure 2b for the three morphologies. We also show the percent Pb decrease for the ICP data (Figure 2b, red squares). For smaller diameters, the cuboctahedron model approximately reproduces our data, while at larger sizes the measured data are significantly lower and begin to approach the truncated cube. These observations can be explained by a sphere-to-cube transition that PbSe QDs are known to undergo and that the exact morphology of the QDs likely deviates from any of the these model shapes. Finally, we can also analyze the EDT-treated PbSe QD films in a similar manner and find that $f = 0.25$ (green dashed line), suggesting a 75% anion enrichment of the QD surfaces.

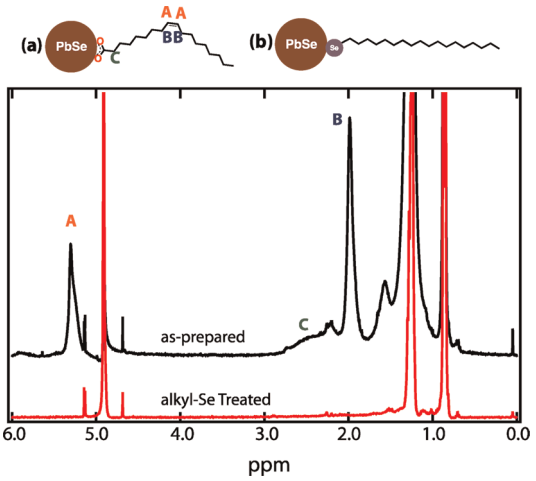

Figure 3. NMR spectra in $CDCl_3$ of as-prepared and alkylselenide-treated 4.7 nm PbSe with dibromomethane (δ ~4.9 ppm) as an internal standard.

Following exchange with alkylselenol, ^{1}H NMR spectroscopy was performed to determine the efficacy of exchange. NMR spectra of as-prepared PbSe QDs show three characteristic resonances (Figure 3a). The most distinctive peak, indicating the presence of oleate, has a chemical shift of 5.34 ppm, which corresponds to the olefinic protons on the internal C—C double bond (Figure 3a, region A). The second characteristic oleate resonance is at 2 ppm, corresponding to the methylene groups adjacent to the C—C double bond (Figure 3a, region B). Finally a broad resonance between 2 and 3 ppm is observed, corresponding to the two protons closest to the carboxylic acid group of oleic acid (Figure 3a, region C). For full assignment of oleate peaks, see Supporting Information Figure S3.

The ^{1}H NMR spectrum recorded following treatment and washing of 4.7 nm QDs indicates a quantitative exchange of oleate for the alkylselenide ligand. The characteristic oleate resonances due to the unsaturation of the alkyl chain (5.34 ppm) are now absent, and the only remaining peaks are those in the region between 1 and 3 ppm, corresponding to the saturated alkyl chains of the bound alkylselenide (Figure 3b). Similar investigation of two additional alkylselenide-treated QD samples (7.9 and 2.3 nm) exhibited the same result: absence of the olefinic proton peaks. In addition, IR spectroscopy confirmed the removal of oleate from the surface and revealed a new absorption band at ~500 cm^{-1} indicative of a Se—C bond,[30] which

also confirms the presence of alkylselenide (see Supporting Information S4 and S5).

The alkylselenol ligand should react in a 1:1 fashion *via* proton exchange with the existing bound oleate ligands on the QD surface. Therefore, the increase in overall Se content in the QDs following treatment with alkylselenol indicates that we need to more carefully consider the QD−oleate interaction. DFT calculations demonstrated that weakly binding carboxylic acid can bind to the stoichiometric {100} facets, while oleate anion predominates on the {111} surfaces.[16] It is reasonable to suggest that these weakly adsorbed, but not chemically bound, neutral oleic acid ligands would dissociate from the {100} surface in the presence of excess alkylselenol. In this manner, only the {111} surfaces undergo true ligand exchange, and yet all of the surface oleate is removed following exchange. Further, a surface Se anion in the form of the alkylselenide ligand could potentially passivate up to three surface Pb atoms, depending on the QD surface facet. This 3-fold bridging is especially applicable to a surface such as the {111}, where Pb atoms are more prevalent, while there may be bonding to only one or two Pb atoms on a {100} surface. Crystal edges with multiple exposed Pb bonding sites may be even more likely to have single Se anions bridging multiple Pb atoms. Quantitative NMR experiments show 2.97×10^{-6} moles of capping ligand per milligram of QDs for as-prepared samples and 2.30×10^{-6} mol/mg for alkylselenide-treated QDs. This 22% decrease in surface ligand coverage following exchange from oleate to alkylselenide supports our above hypothesis that neutral oleic acid may also be adsorbed to the QD surface. Experiments to further explore these propositions are ongoing.

Optical Properties and Reduced Oxidation Rate. QD films for spectroscopic studies were dropcast from chloroform solution onto a sapphire substrate and sealed under inert atmosphere. For the alkylselenide-capped QDs, the absorbance spectrum shows an initial red-shift in the first excitonic peak of approximately 30 meV compared with films of as-prepared QDs (Figure 4), suggesting an increase in QD diameter of not more than 0.3 nm, less than a monolayer for the QD sizes investigated (1−10 nm).[19,20] For our spectroscopic study, we focused on QDs of intermediate size (4−5 nm), which allows for direct comparison with a recent report describing trends in the PL *versus* temperature that exhibited sensitivity to QD surface composition and quality.[1]

The temperature-dependent PL spectra for as-prepared and alkylselenide-treated QDs before (A, D) and after (B, E) exposure to oxygen are presented in Figure 5. PbSe has a temperature-dependent band gap reported in Figure S5. For this size regime the shift of the absorbance peak for the first exciton peak is on the order of 0.01 eV toward higher energy from 13 to 300 K (see Figure S6). The spectra for as-prepared QDs exhibit a temperature-dependent emission peak shift of 0.1 eV

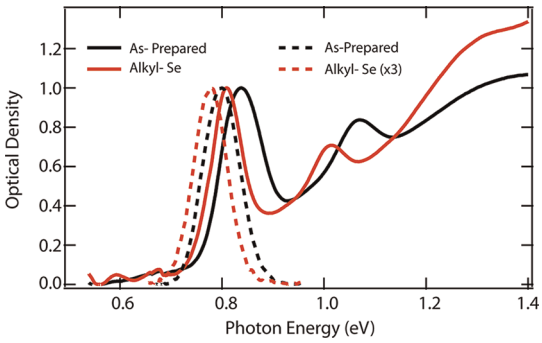

Figure 4. Normalized absorption and photoluminescence spectrum of as-prepared QDs with diameter of 4.7 nm before and after alkylselenide treatment. The solid lines are for the absorption, while the dashed lines are for emission. After treatment the emission efficiency decreases by ~3.

through this temperature range. Since the PL shift is much larger than the absorbance shift, we implement a model invoking two distinct but interacting emitting species. The excited states are denoted **A** and **B**, respectively, and are depicted in the energy band diagrams in Figure 6, where **B** is the conduction band and **A** is a lower energy electron trap. Emission from **A** occurs at low temperature, and the population of carriers gradually flows into state **B** as the temperature is increased. A recent investigation of oleate-capped PbSe QDs studied the thermal equilibrium between states **A** and **B** for various QD sizes and developed a phenomenological model to describe the kinetics of the various relaxation pathways.[1] The effect of oxidation was also included in this model, and it was demonstrated that upon oxidation of as-prepared QDs, an additional relaxation pathway is introduced and is depicted by pathway **Ox**, as shown in Figure 6. Upon ligand exchange of as-made QDs with alkylselenide, emission from states **A** and **B** is still observed, and we deduce the formation of a new nonradiative decay pathway identified as a hole-trap level, **H**, which we propose to lie near the valence band.

A plot of the integrated PL intensity ($I_{PL}(T)$), which is proportional to the PLQY, *versus* temperature is given for each sample (Figure 5 C,F). Prior to air exposure, $I_{PL}(T)$ plots for as-prepared and alkylselenide-capped QDs are quite similar, though measurable decreases in the room-temperature PLQYs (ranging between a factor of 0.3 and 0.5) are observed for alkylselenide-treated particles. This decrease in PLQY at room temperature is attributed to the creation of a low-lying intrinsically dark state associated with the addition of surface selenium, as was shown in similar work in CdSe.[26] According to our model, some photoexcited holes become trapped in **H**, leading to the significant reduction in the overall PLQY at room temperature compared to as-prepared QDs. Partial alkylselenide termination at the surface may introduce acceptor-like states near the valence band intrinsic to the large, electron-rich Se_{surf} groups. This is similar to P_{surf}-based traps in InP and Se_{surf}-based traps in CdSe.[26,31]

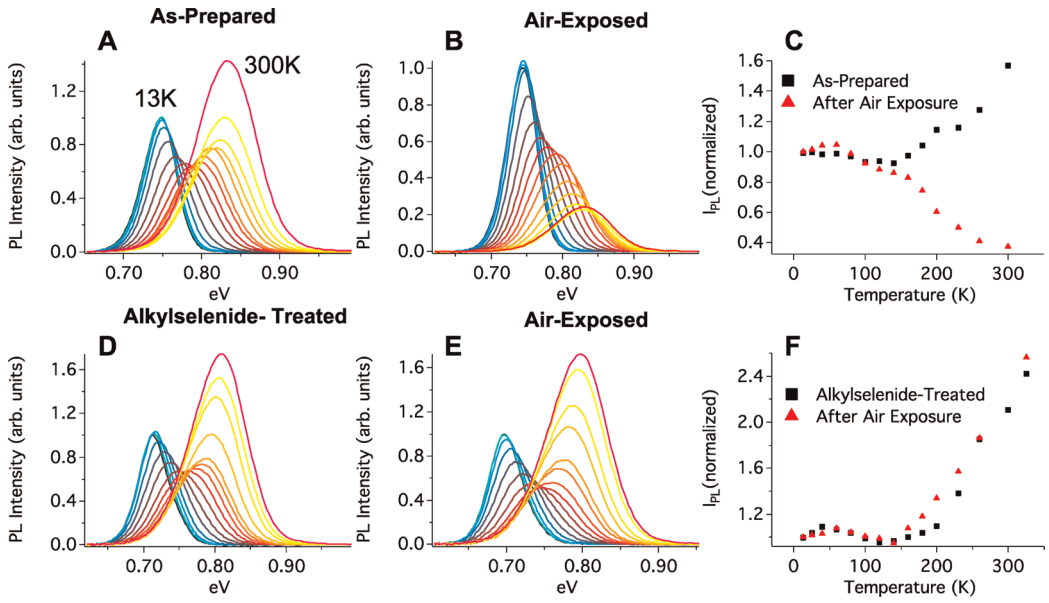

Figure 5. (A, B, D, E) Temperature-dependent photoluminescence data for as-prepared and alkylselenide-treated 4.7 nm PbSe QDs before and after oxygen exposure. (C) Integrated PL intensity *vs* temperature plot for pristine and air-exposed 4.7 nm QDs. (F) Integrated PL intensity *vs* temperature plot for alkylselenide-treated and air-exposed alkylselenide-treated 4.7 nm QDs.

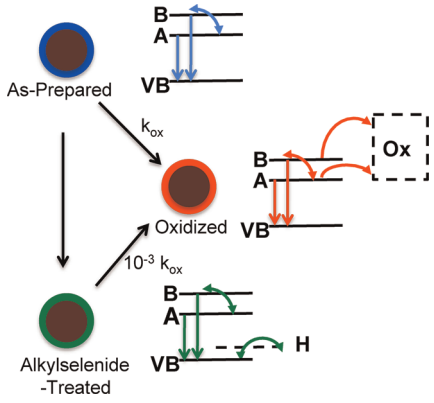

Figure 6. Relaxation pathways for excited populations in as-prepared, oxidized, and alkylselenide-treated QDs. Solid lines indicate bright states, while dashed lines signify dark states. Each QD type exhibits population flow between states B and A, as well as radiative decay from bands A and B to the valence band (VB).

Although the $I_{PL}(T)$ curves for as-prepared and alkylselenide-capped QDs are similar, noticeable qualitative differences in the shape support the expected change in surface-influenced photophysics. For example, a small rise in $I_{PL}(T)$ occurs at low temperature in alkylselenide QDs but not in as-prepared QD samples (Figure 7). This rise is consistent with the thermal activation of holes from the dark state **H** to the **VB**, where the radiative transition **A**→**VB** can occur.[1] This characteristic rise in I_{PL} at low temperatures is also apparent in QDs treated only with elemental Se *via* TOP-Se (data not shown), and the rise is more pronounced for smaller QDs (2−3 nm), as shown in Figure S7. The more pronounced rise for smaller QDs can be correlated with the amount of Se added to the surface (see Figure 2a). In addition to a rise in I_{PL}, the steeper slope observed in the $I_{PL}(T)$ above 150 K for alkylselenide QDs *versus* as-prepared samples is indicative of a lower density of **A** states (identified with excess surface Pb) pushing the **A**→**B** equilibrium more strongly toward **B** with increased temperature. A quantitative estimate of state density changes would rely on a more detailed model beyond the scope of this study; however, the qualitative trends strongly suggest that the photophysics is altered by the replacement of Pb-oleate with alkylselenide.

To further support the validity of our hypotheses regarding the normalized $I_{PL}(T)$ curves, we employ here a simulation that is based on the general phenomenological model presented by Chappell *et al*. In our case, the relatively subtle trends prevented an accurate least-squares fit to the data without significant parameter covariance. Thus this simulation depicts how the relevant trends in our data arise as a function of varying those parameters related to surface trap states. The integrated PL is calculated from

$$I_{PL}(T) = \frac{1}{(1 + h\exp(-E_h/kT))} \times \left\{ \frac{1}{(1 + c\exp(\Delta G/kT))(1 + s(\exp(E_{ph}/kT) - 1)^{-m})} + \Phi_b\left(1 - \frac{1}{1 + c\exp(\Delta G/kT)}\right)\right\}$$

where Φ_b is the ratio of the radiative efficiency of state **B** to state **A**, ΔG is the energy gap between states **A** and **B**, and E_h is the energy of activation between the hole-trap **H** and the valence band. E_{ph}, s, and m are parameters relating to carrier−phonon coupling,[32] which are floated to fit I_{PL} curves for untreated QDs and then are fixed at the same values for alkylselenide-treated QDs, upon the expectation that these terms are independent of surface

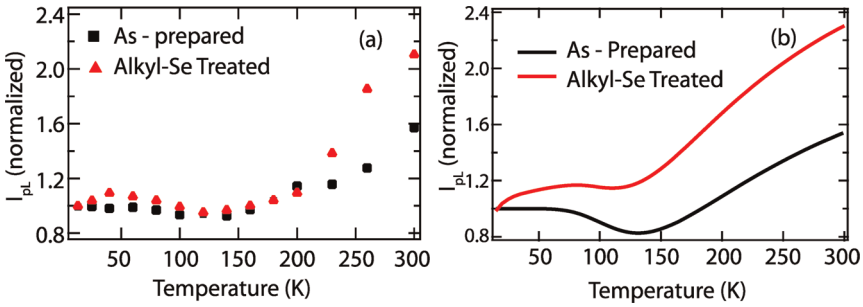

Figure 7. (a) Integrated PL intensity *vs* temperature plot for as-prepared and alkylselenide-treated 4.7 nm QDs, showing characteristic rise in I_{PL} at low T for alkylselenide-treated QDs and steeper slope above 150 K. (b) Simulated data set that qualitatively matches the measured data. The simulation is described in the text. The red curve was scaled by a factor of 2.5.

TABLE 1. Fit Parameters As They Vary with Changing Surface Chemistry

	m	Φ_B	c	ΔG (meV)	s	E_{ph}(meV)	h	E_h(meV)
as-prepared	4	4	2	−30.3	0.18	5.2	0	0
alkylselenide-treated	4	4	3	−30.3	0.18	5.2	2.5	0.35

treatment. We tentatively assign **H** to a hole-trap level on the basis of the consideration discussed below. c represents a statistical weighting of **A** and **B** states, and h is related to the statistical distribution of VB and hole-trap states **H**. The higher the values of h, the stronger the influence of hole traps. With all other parameters remaining approximately equal, an increase in h leads to the rise in $I_{PL}(T)$ at low temperature and also the overall smaller value of $I_{PL}(T)$ at room temperature, as evidenced in the simulated data in Figure 7b. How each of these parameters changes in our simulation is shown in Table 1. Besides increasing the values of hole-trap parameters h and E_h, a higher value of c for alkylselenide-treated QDs is also needed to produce the larger slope in I_{PL} at higher temperatures, as seen in the experimental data. This is indicative of a lower relative ratio of **A**:**B** concentrations, presumably from passivating some fraction of the electron traps **A** that arise from excess Pb.

As-prepared and alkylselenide-capped QD films react very differently following 1 min of air exposure. As-prepared samples exhibit quenching of PL intensity at temperatures above 150 K due to the introduction of oxygen-based nonradiative trap states, as depicted in our model as **Ox** (Figure 4).[1] This characteristic quenching of PL intensity for oleate-capped Pb salts is not observed for alkylselenide-capped QDs, even after exposure times of 90 min. This result is most likely due to the formation of a more stable Pb_{surf}—Se bond, which passivates Pb_{surf} sites and impedes oxidation over time scales in which as-prepared QDs undergo oxidative damage. Upon air exposure for multiple hours, the characteristic decay in PL intensity at $T > 150$ K is observed, signifying surface oxidation. Nevertheless, the rate of PL quenching is slowed by at least 2 orders of magnitude for alkylselenide-capped QDs.

CONCLUSIONS

Following treatment with the alkylselenide ligand, QDs exhibit two new properties: (1) they resist short-term oxidation and (2) they adopt the expected photophysical properties of a more stoichiometric QD. The former is an interesting practical result that may allow for short-term processing or characterizing of PbSe QDs in the presence of oxygen, while the latter suggests that controlling the surface composition allows for engineering of specific dynamical behavior. Surface composition naturally changes with QD size, and thus surface chemistry is usually an uncontrolled variable in size-dependent studies. Trends for various properties that are believed to be dependent on QD size, such as PLQY[33] and electron/hole mobilities,[4] may at least in part be dictated more definitively with surface composition. Since surface effects can dominate both the photophysical and electrical properties of QDs, tailoring of the surface to enhance beneficial properties, such as improved transport, is a potentially powerful tool.

The surface exchanges presented here can easily be translated to other Pb-chalcogenide systems and to various Pb-chalcogenide nanostructures, with the end goal of a more robust QD surface. This type of surface passivation holds promise to enable further exploration of the effects of surface modification on photophysical and materials properties, including carrier dynamics. Consequences of this surface treatment methodology for carrier mobility and doping in electronically coupled QD films will be investigated employing similar alkyl-chalcogenide compounds with tunable ligand lengths.

MATERIALS AND METHODS

Materials. All chemicals were used as received without further purification. Selenium (99.99%), sodium borohydride (99.99%), oleic acid (90%), 1-iodooctadecane (90%), diphenylphosphine (DPP, 98%), trioctylphosphine (TOP 90%), anhydrous ethanol, hexane, and tetrachloroethylene (TCE 99.9%) were purchased from Aldrich and used as received. Lead oxide

(99.999%) was purchased from Alfa Aesar. The diselenide and selenol reagents were prepared using dry and/or degassed solvents and standard Schlenk techniques under a nitrogen atmosphere. *Warning: A small amount of H_2Se is released in the early stages of these reactions*. Due to the high toxicity of this volatile compound, all manipulations should be performed in a fume hood with adequate ventilation. In addition, excess nitrogen flow from these reactions was bubbled through a 5 wt % aqueous lead acetate solution to trap the volatile H_2Se as solid PbSe.

Synthesis of Dioctadecyl Diselenide (1). This preparation was adapted from a literature procedure of similar dialkyl diselenides.[27] Cooled, degassed absolute ethanol (50 mL) was added *via* cannula to a cooled (0 °C) solid mixture of Se metal (1.0 g, 12.7 mmol) and sodium borohydride (0.34 g, 8.9 mmol) under nitrogen. The reaction bubbled vigorously for about 1 min (releasing a small amount of H_2Se) and changed to dark red in color, indicative of the formation of Na_2Se_2. After 15 min at 0 °C, the dark red solution was heated at reflux for 30 min to complete the formation of Na_2Se_2. After cooling to room temperature, a solution of 1-iodooctadecane (3.4 g, 8.9 mmol) in THF (15 mL) was added dropwise *via* syringe. After 15 min at room temperature, the reaction was heated at reflux for 2 h. The reaction was then cooled and acidified *via* the addition of *ca*. 2 mL of acetic acid. The yellow product began to precipitate from the solution, but was redissolved with chloroform (40 mL). To ensure that any trace H_2Se was fully expelled from the reaction flask, nitrogen was bubbled directly through the reaction mixture for 15 min. The solution was then extracted with water (2 × 30 mL), dried over $MgSO_4$, and filtered. The solvent was removed *in vacuo*, leaving analytically pure, solid yellow product (2.43 g, 82%). ^{1}H NMR (400 MHz, chloroform-*d*, 20 °C): δ 2.91 (t, 2H), 1.72 (pent, 2H), 1.26 (m, 30H), 0.88 (t, 3H). $^{13}C\{^1H\}$ NMR (100 MHz, chloroform-*d*, 20 °C): δ 31.9, 31.0, 30.3, 29.7, 29.6, 29.5, 29.4, 29.1, 22.7, 14.1. Anal. Calcd for $C_{36}H_{74}Se_2$: C, 65.03; H, 11.22. Found: C, 64.63; H, 10.91.

Synthesis of Octadecylselenol (2). Cooled, degassed absolute ethanol (20 mL) was added *via* cannula to a cooled (0 °C) solid mixture of Se metal (0.60 g, 7.6 mmol) and sodium borohydride (0.32 g, 8.4 mmol) under nitrogen. A pale orange-red color developed over *ca*. 15 min at 0 °C. The reaction was allowed to warm to room temperature and stirred for 30 min. A solution of 1-iodooctadecane (2.9 g, 7.6 mmol) in THF (15 mL) was added dropwise *via* syringe. The reaction was stirred at 30 °C for 90 min, followed by cooling to 0 °C and quenching with dilute aqueous HCl. Chloroform (15 mL) was added, and nitrogen was bubbled through the solution to remove any trace H_2Se. The solution was extracted with water (2 × 30 mL), dried over $MgSO_4$, and filtered. The solvent was removed *in vacuo*, and the off-white product was stored in a glovebox. The crude product (2.0 g, 79%) is 85% pure by ^{1}H NMR analysis. Analytically pure, colorless product (1.3 g, 51%) can be isolated via sublimation (120 °C, 0.005 mmHg). ^{1}H NMR (400 MHz, chloroform-*d*, 20 °C): δ 2.58 (q, 2H), 1.70 (pent, 2H), 1.26 (m, 30H), 0.88 (t, 3H), −0.69 (t, 1H, Se-*H*). $^{13}C\{^1H\}$ NMR (100 MHz, chloroform-*d*, 20 °C): δ 34.0, 31.9, 29.7, 29.6, 29.5, 29.4, 29.0, 22.7, 17.7, 14.1. Anal. Calcd for $C_{18}H_{38}Se$: C, 64.83; H, 11.49. Found: C, 65.13; H, 11.23.

Synthesis of Alkylselenide-Capped PbSe QDs *via* Two-Injection Method. A solution of $Pb(oleate)_2$ was prepared by heating PbO (0.25 g, 1.12 mmol) with oleic acid (0.633 g, 2.24 mmol) in 1-octadecene (8 mL). This solution was heated to 100 °C under vacuum for 10 min before being degassed under N_2 for 30 min. The reaction temperature was increased to 160 °C before the first injection of 1 M TOP-Se (2.24 mL) containing diphenylphosphine (0.035 g, 0.188 mmol). A second solution containing dioctadecyl diselenide (0.037 g 0.025 mmol) in a minimum amount of $CHCl_3$ was injected 25 s after the first injection. The reaction was heated continuously for another 20 s following the second injection, at which point the reaction was removed from heating and quenched with 10 mL of hexane. The resulting particles were washed twice by precipitation with EtOH and isolated by centrifugation.

Synthesis of Alkylselenide-Capped PbSe QDs *via* Ligand Exchange. PbSe QDs were prepared according to previously reported methods.[23,34] For exchange using **1**, 250 mg of QDs was dispersed in 7 mL of hexane, followed by the addition of **1** (0.035 g, 0.048 mmol) and DPP (0.003 g, 0.016 mmol). This solution was allowed to stir for 2 days, after which the QDs were observed to precipitate from solution. The particles were washed twice with hexane, isolated by centrifugation, and redispersed in $CHCl_3$. Similarly, for exchange using **2**, the QDs (0.250 g) were dispersed in 7 mL of hexane and **2** (0.009 g, 0.027 mmol) was added. Upon gentle stirring, the QDs precipitated from solution within minutes. The particles were washed twice with hexane, isolated by centrifugation, and redispersed in $CHCl_3$.

Film Preparation. Films were dropcast onto a sapphire substrate from a solution of ~5−10 mg/mL of QDs in a 4:1 hexane/octane solution. The resulting films were macroscopically uniform and essentially opaque at the excitation wavelength (488 nm) and were estimated to be greater than 100 nm thick. Films were sealed in a copper gasket with an O-ring between a second sapphire window. For air exposure studies, the airtight seal on the sample holder was broken and the films were exposed to ambient air in the dark. The films were resealed in the glovebox before PL was measured again.

Characterization. Elemental analyses for treated QDs were performed by Galbraith Laboratories (Knoxville, TN, USA) using inductively coupled plasma optical emission spectroscopy. Elemental analyses for compounds **1** and **2** were performed by Huffman Laboratories (Golden, CO, USA). NMR experiments were performed on a Varian Inova 400 MHz spectrometer. Prior to ligand exchange, NMR spectra were recorded using toluene-d_8 as solvent, which allowed us to distinguish between free and bound oleic acid. High-resolution magic angle spinning experiments were performed. All spectra of exchanged QDs were taken in chloroform-*d* due to their insolubility in toluene. High-resolution transmission electron microscopy was carried out using a Philips CM 200 at 120 kV. Fourier transform infrared (FTIR) absorbance spectra were recorded on a Thermo-Nicolet 6700 FTIR spectrometer in transmission mode with a resolution of 4 cm^{-1}. For photoluminescence films were left stationary in the PL system during the measurement of a sample across the entire temperature range, which was always collected beginning at 13 K and warming to 325 K. No significant difference was noted for data collected while cooling from 325 to 13 K. The sample was allowed to fully equilibrate at each temperature (*i.e.*, until the PL spectrum remained constant, about 5−10 min). PL spectra were recorded under vacuum (<10^{-5} Torr) in a closed-loop He cryostat. Films were excited with 10−20 mW Ar ion laser excitation at 488 nm, mechanically chopped at 1 kHz, and unfocused (spot size roughly 3 mm diameter). The resulting PL spectra were detected with an amplified InSb photodiode routed to a lock-in amplifier. Spectra were corrected for monochromator and detector efficiencies using a calibrated lamp. Representative temperature-dependent PL spectra were reported for each sample set, and these spectra were reproducible within 7% error. This error is most probably due to inhomogeneities in film surfaces between samples.

Conflict of Interest: The authors declare no competing financial interest.

Acknowledgment. We gratefully acknowledge support from the Solar Photochemistry program within the Division of Chemical Sciences, Geosciences, and Biosciences in the Office of Basic Energy Sciences of the U.S. Department of Energy. DOE funding to NREL was provided under contract no. DE-AC36-08GO28308. We also thank S. Nanayakkara, E. Gjersing, and N. Neale for helpful discussions.

Supporting Information Available: Synthetic details of **1** and **2** and ligand exchange, elemental analysis and TEM, experimental details of PL measurements, and absorbance and FTIR spectra for as-prepared and alkylselenide-treated PbSe QDs. This material is available free of charge *via* the Internet at http://pubs.acs.org

REFERENCES AND NOTES

1. Chappell, H. E.; Hughes, B. K.; Beard, M. C.; Nozik, A. J.; Johnson, J. C. Emission Quenching in PbSe Quantum Dot Arrays by Short-Term Air Exposure. *J. Phys. Chem. Lett.* **2011**, *2*, 889–893.

2. Lingley, Z.; Lu, S.; Madhukar, A. A High Quantum Efficiency Preserving Approach to Ligand Exchange on Lead Sulfide Quantum Dots and Interdot Resonant Energy Transfer. *Nano Lett.* **2011**, *11*, 2887–2891.
3. Tang, J.; Brzozowski, L.; Barkhouse, D. A. R.; Wang, X.; Debnath, R.; Wolowiec, R.; Palmiano, E.; Levina, L.; Pattantyus-Abraham, A. G.; Jamakosmanovic, D.; *et al.* Quantum Dot Photovoltaics in the Extreme Quantum Confinement Regime: The Surface-Chemical Origins of Exceptional Air- and Light-Stability. *ACS Nano* **2010**, *4*, 869–878.
4. Liu, Y.; Gibbs, M.; Puthussery, J.; Gaik, S.; Ihly, R.; Hillhouse, H. W.; Law, M. Dependence of Carrier Mobility on Nanocrystal Size and Ligand Length in PbSe Nanocrystal Solids. *Nano Lett.* **2010**, *10*, 1960–1969.
5. Midgett, A. G.; Hillhouse, H. W.; Hughes, B. K.; Nozik, A. J.; Beard, M. C. Flowing versus Static Conditions for Measuring Multiple Exciton Generation in PbSe Quantum Dots. *J. Phys. Chem. B* **2010**, *114*, 17486–17500.
6. Sykora, M.; Koposov, A. Y.; McGuire, J. A.; Schulze, R. K.; Tretiak, O.; Pietryga, J. M.; Klimov, V. I. Effect of Air Exposure on Surface Properties, Electronic Structure, and Carrier Relaxation in PbSe Nanocrystals. *ACS Nano* **2010**, *4*, 2021–2034.
7. Semonin, O. E.; Luther, J. M.; Choi, S.; Chen, H.-Y.; Gao, J.; Nozik, A. J.; Beard, M. C. Peak External Photocurrent Quantum Efficiency Exceeding 100% via MEG in a Quantum Dot Solar Cell. *Science* **2011**, *334*, 1530–1533.
8. Hillhouse, H. W.; Beard, M. C. Solar cells from colloidal nanocrystals: Fundamentals, Materials, Devices, and Economics. *Curr. Opin. Colloid Interface Sci.* **2009**, *14*, 245–259.
9. Kramer, I. J.; Sargent, E. H. Colloidal Quantum Dot Photovoltaics: A Path Forward. *ACS Nano* **2011**, *5*, 8506–8514.
10. Schliehe, C.; Juarez, B. H.; Pelletier, M.; Jander, S.; Greshnykh, D.; Nagel, M.; Meyer, A.; Foerster, S.; Kornowski, A.; Klinke, C.; *et al.* Ultrathin PbS Sheets by Two-Dimensional Oriented Attachment. *Science* **2010**, *329*, 550–553.
11. Lovingood, D. D.; Achey, R.; Paravastu, A. K.; Strouse, G. F. Size- and Site-Dependent Reconstruction in CdSe QDs Evidenced by $^{77}Se\{^{1}H\}$ CP-MAS NMR Spectroscopy. *J. Am. Chem. Soc.* **2010**, *132*, 3344–3354.
12. Gai, Y.; Peng, H.; Li, J. Electronic Properties of Nonstoichiometric PbSe Quantum Dots from First Principles. *J. Phys. Chem. B* **2009**, *113*, 21506–21511.
13. Petkov, V.; Moreels, I.; Hens, Z.; Ren, Y.PbSe Quantum Dots: Finite, off-Stoichiometric, and Structurally Distorted. *Phys. Rev. B* **2010**, *81*, 241304.
14. Fang, C.; van Huis, M. A.; Vanmaekelbergh, D.; Zandbergen, H. W. Energetics of Polar and Nonpolar Facets of PbSe Nanocrystals from Theory and Experiment. *ACS Nano* **2010**, *4*, 211–218.
15. Dai, Q.; Wang, Y.; Li, X.; Zhang, Y.; Pellegrino, D. J.; Zhao, M.; Zou, B.; Seo, J.; Wang, Y.; Yu, W. W. Size-Dependent Composition and Molar Extinction Coefficient of PbSe Semiconductor Nanocrystals. *ACS Nano* **2009**, *3*, 1518–1524.
16. Argeri, M.; Fraccarollo, A.; Grassi, F.; Marchese, L.; Cossi, M. Density Functional Theory Modeling of PbSe Nanoclusters: Effect of Surface Passivation on Shape and Composition. *J. Phys. Chem. B* **2011**, *115*, 11382–11389.
17. Voznyy, O. Mobile Surface Traps in CdSe Nanocrystals with Carboxylic Acid Ligands. *J. Phys. Chem. B* **2011**, *115*, 15927–15932.
18. Choi, J. J.; Bealing, C. R.; Bian, K.; Hughes, K. J.; Zhang, W.; Smilgies, D.-M.; Hennig, R. G.; Engstrom, J. R.; Hanrath, T. Controlling Nanocrystal Superlattice Symmetry and Shape-Anisotropic Interactions through Variable Ligand Surface Coverage. *J. Am. Chem. Soc.* **2011**, *133*, 3131–3138.
19. Moreels, I.; Lambert, K.; De Muynck, D.; Vanhaecke, F.; Poelman, D.; Martins, J. C.; Allan, G.; Hens, Z. Composition and Size-Dependent Extinction Coefficient of Colloidal PbSe Quantum Dots. *Chem. Mater.* **2007**, *19*, 6101–6106.
20. Smith, D. S., D. K.; Luther, J. M.; Semonin, O. E.; Nozik, A. J.; Beard, M. C. Tuning the Synthesis of Ternary Lead Chalcogenide Quantum Dots by Balancing Precursor Reactivity. *ACS Nano* **2011**, *5*, 183–190.
21. Moreels, I.; Fritzinger, B.; Martins, J. C.; Hens, Z. Surface Chemistry of Colloidal PbSe Nanocrystals. *J. Am. Chem. Soc.* **2008**, *130*, 15081–15086.
22. Bealing, C. R.; Baumgardner, W. J.; Choi, J. J.; Hanrath, T.; Hennig, R. G. Predicting Nanocrystal Shape through Consideration of Surface-Ligand Interactions. *ACS Nano* **2012**, *6*, 2118–2127.
23. Law, M.; Luther, J. M.; Song, O.; Hughes, B. K.; Perkins, C. L.; Nozik, A. J. Structural, Optical, And Electrical Properties of PbSe Nanocrystal Solids Treated Thermally or with Simple Amines. *J. Am. Chem. Soc.* **2008**, *130*, 5974–5985.
24. Allgaier, R. S.; Scanlon, W. W. Mobility of Electrons and Holes in PbS, PbSe and PbTe between Room Temperature and 4.2 K. *Phys. Rev.* **1958**, *111*, 1029–1037.
25. Franceschetti, A. Structural and Electronic Properties of PbSe Nanocrystals from First Principles. *Phys. Rev. B* **2008**, *78*, 075418.
26. Mulvaney, P.; Jasieniak, J. From Cd-rich to Se-rich—The Manipulation of CdSe Nanocrystal Surface Stoichiometry. *J. Am. Chem. Soc.* **2007**, *129*, 2841–2848.
27. Klayman, D. L.; Griffin, T. S. Reaction of Selenium with Sodium-Borohydride in Protic Solvents-Facile Method for Introduction of Selenium into Organic Molecules. *J. Am. Chem. Soc.* **1973**, *95*, 197–200.
28. Koval, I. V. Chemistry of Disulfides. *Usp. Khim.* **1994**, *63*, 776–792.
29. Bian, K.; Choi, J. J.; Kaushik, A.; Clancy, P.; Smilgies, D.-M.; Hanrath, T. Shape-Anisotropy Driven Symmetry Transformations in Nanocrystal Superlattice Polymorphs. *ACS Nano* **2011**, *5*, 2815–2823.
30. Benidar, A.; Khater, B.; Guillemin, J.; Gamez, J.; Yanez, M. Gas-Phase Infrared Spectra of Vinyl Selenol and Vinyl Tellurol. *J. Phys. Chem. A* **2009**, *113*, 12857–12863.
31. Poles, E.; Selmarten, D. C.; Micic, O. I.; Nozik, A. J. Anti-Stokes Photoluminescence in Colloidal Semiconductor Quantum Dots. *Appl. Phys. Lett.* **1999**, *75*, 971–973.
32. Morello, G.; De Giorgi, M.; Kudera, S.; Manna, L.; Cingolani, R.; Anni, M. Temperature and Size Dependence of Nonradiative Relaxation and Exciton-Phonon Coupling in Colloidal CdTe Quantum Dots. *J. Phys. Chem. B* **2007**, *111*, 5846–5849.
33. Semonin, O. E.; Johnson, J. C.; Luther, J. M.; Midgett, A. G.; Nozik, A. J.; Beard, M. C. Absolute Photoluminescence Quantum Yields of IR-26 Dye, PbS, and PbSe Quantum Dots. *J. Phys. Chem. Lett.* **2010**, *1*, 2445–2450.
34. Bawendi, M. G.; Steckel, J. S.; Yen, B. K. H.; Oertel, D. C. On the Mechanism of Lead Chalcogenide Nanocrystal Formation. *J. Am. Chem. Soc.* **2006**, *128*, 13032–13033.